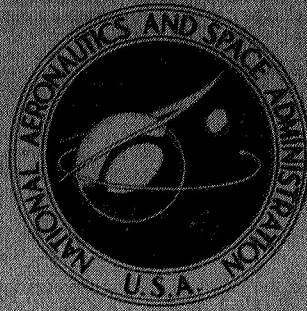


NASA TECHNICAL  
MEMORANDUM



NASA TM X-2700

NASA TM X-2700

CASE FILE  
COPY

PRELIMINARY STUDY OF  
A WALL-STABILIZED CONSTRICTED ARC

*by Randolph A. Graves and William L. Wells*

*Langley Research Center*

*Hampton, Va. 23365*

1. Report No. NASA TM X-2700	2. Government Accession No.	3. Recipient's Catalog No.	
4. Title and Subtitle PRELIMINARY STUDY OF A WALL-STABILIZED CONSTRICTED ARC		5. Report Date February 1973	6. Performing Organization Code
		8. Performing Organization Report No. L-8631	
7. Author(s) Randolph A. Graves and William L. Wells		10. Work Unit No. 502-27-01-01	11. Contract or Grant No.
9. Performing Organization Name and Address NASA Langley Research Center Hampton, Va. 23365		13. Type of Report and Period Covered Technical Memorandum	
		14. Sponsoring Agency Code	
12. Sponsoring Agency Name and Address National Aeronautics and Space Administration Washington, D.C. 20546		15. Supplementary Notes	
16. Abstract  An iterative, implicit, finite-difference numerical technique is described which is suitable for obtaining solutions to the governing equations for a gas flowing in an axially symmetric constricted-arc heater. The method is shown to provide adequate solutions for three cases of simple pipe flows found in the literature, and for flow in a constricted-arc heater by direct comparison with experimental data. The comparison with arc-heater data includes static pressure, arc voltage, and wall heat flux, all as a function of axial location, and a radial temperature profile at one axial station. The arc-heater data were taken with air as the test gas at a heater inlet pressure of approximately 0.40 atm and two flow rates of 2.2 and 4.8 g/sec. The arc currents investigated were between 377 and 584 amperes.  A brief description of the experimental apparatus is included.			
17. Key Words (Suggested by Author(s)) Arc jet Viscous flow Plasma flow Boundary layer Heat transfer Implicit solution		18. Distribution Statement Unclassified - Unlimited	
19. Security Classif. (of this report) Unclassified	20. Security Classif. (of this page) Unclassified	21. No. of Pages 34	22. Price* \$3.00

## PRELIMINARY STUDY OF A WALL-STABILIZED CONSTRICTED ARC

By Randolph A. Graves and William L. Wells  
Langley Research Center

### SUMMARY

An iterative, implicit, finite-difference numerical technique is described which is suitable for obtaining solutions to the governing equations for a gas flowing in an axially symmetric constricted-arc heater. The method is shown to provide adequate solutions for three cases of simple pipe flows found in the literature, and for flow in a constricted-arc heater by direct comparison with experimental data. The comparison with arc-heater data includes static pressure, arc voltage, and wall heat flux, all as a function of axial location, and a radial temperature profile at one axial station. The arc-heater data were taken with air as the test gas at a heater inlet pressure of approximately 0.40 atm and two flow rates of 2.2 and 4.8 g/sec. The arc currents investigated were between 377 and 584 amperes.

A brief description of the experimental apparatus is included.

### INTRODUCTION

A study of the axially symmetric constricted-arc column was undertaken in conjunction with a spectroscopic study of the spectral dependence of radiant heat transfer from hot gases. In addition to the present specific application of the wall-stabilized constricted arc, there is currently considerable interest in the use of the arc configuration for materials studies, plasma dynamics, and so forth. The constricted arc is a device in which a gas flows parallel to the axis of an electrical discharge and is confined by the cooled walls of the tube. The temperatures attained within the arc column are of order  $10^4$  K and the processes which occur are highly complex and interrelated. Proper utilization of the constricted arc requires a knowledge of the spatial distribution of fluid mechanic, thermal, and electromagnetic variables. Toward this goal, many investigators have put forth simplified analytical methods which for a variety of reasons do not describe with sufficient accuracy the complex phenomena occurring within the hot arc column. (Refs. 1 and 2 give an excellent review of previous work.)

Representative of the existing numerical techniques found in the literature are those presented in references 2 and 3. Both these methods have limitations which detract from their usefulness. Reference 2 uses an implicit method along the lines of a Crank-Nicholson

approach which results in instabilities at arc currents greater than 300 amperes and/or gas flow rates greater than 3 g/sec. Reference 3 uses a fully explicit numerical technique in which the axial step size is constrained to small values by the stability criterion. The development described herein is fully implicit and should be inherently more stable.

The present work on the constricted-arc section was performed to provide a numerical tool for the description of the pertinent variables within the arc column. The numerical technique is an iterative, implicit, finite-difference method which describes the axial and radial fluid mechanic and thermal variables. This report will describe both the analysis and the experimental apparatus and make comparisons between some experimental measurements and computed values.

### SYMBOLS

$C_r$	nodal spacing constant
$c_p$	specific heat at constant pressure, J/kg-K
$E_z$	axial voltage gradient, V/m
$F, f$	any mathematical function
$H$	total enthalpy, J/kg
$h$	static enthalpy, J/kg
$I$	electrical current, amperes
$k$	thermal conductivity, W/m-K
$l$	mixing length, m
$M$	total number of nodal points
$\dot{m}$	air mass-flow rate, g/sec
$N_{Nu}$	Nusselt number, $N_{Nu} = \frac{2r_w q_w}{k(T_w - T_m)}$
$N_{Pr}$	Prandtl number

$N_{Re}$	Reynolds number, $\frac{\rho u 2r_w}{\mu}$
$p$	pressure, atm (1 atm = 101.3 kN/m <sup>2</sup> )
$Q$	radiated power, W/m <sup>3</sup>
$q$	heat flux, W/m <sup>2</sup>
$R$	nondimensional radial distance
$r$	radial distance, m
$T$	temperature, K
$T_m$	bulk mean temperature, $T_m = 2 \int_0^1 UTR \, dR$ , K
$U$	nondimensional axial velocity
$\bar{U}_m$	mean axial velocity, $\bar{U}_m = 2 \int_0^1 UR \, dR$
$u$	axial velocity, m/sec
$V$	nondimensional radial velocity
$v$	radial velocity, m/sec
$Z$	compressibility factor
$z$	axial distance, m
$\gamma$	electrical conductivity, mhos/m
$\epsilon$	eddy viscosity, m <sup>2</sup> /sec
$\theta$	temperature, $T/T_{m,0}$
$\mu$	dynamic viscosity, N-sec/m <sup>2</sup>
$\bar{\mu}_p$	Planck mean absorption coefficient, 1/m

$\rho$	density, kg/m <sup>3</sup>
$\sigma$	Stefan-Boltzmann constant, W/m <sup>2</sup> -K <sup>4</sup>
$\tau$	shear stress, N/m <sup>2</sup>

Subscripts:

e	effective
h	enthalpy
K	denotes arbitrary grid point in axial direction
m	momentum or mean
N	denotes arbitrary grid point in radial direction
o	entrance condition
t	turbulent
w	wall

A bar over a symbol denotes a nondimensional quantity.

## APPARATUS

### Arc Heater

The arc heater (see fig. 1) was of the wall-stabilized type, which utilizes a constant-diameter constrictor for stabilization and confinement of the arc and gas. The constrictor was 42.4 cm long with an inside diameter of 2.37 cm. The arc attached to a hollow tungsten cathode at the upstream end and to multiple (32) cooled copper anodes in an expansion section just downstream of the constrictor exit. Resistors were in series with the anodes to cause the electrical current to divide evenly to each anode and thereby result in a very quiescent arc. The constrictor was constructed of alternate wafers of ceramic insulators and water-cooled heat conductors (copper). Cooling lines to these wafers were nonconductive so that each wafer was electrically isolated and was allowed to rise to the local arc potential during operation. One special wafer was equipped with a recessed

quartz window which provided a side view of the arc for spectrographic temperature measurements. To avoid rapid oxidation of the tungsten cathode, a very small amount (less than 0.2 percent of the airflow) of argon was introduced into the cathode well.

### Instrumentation

Water and inlet air temperatures were measured with thermocouples; cooling-water flow rates, with turbine flow transducers; pressures, with strain-gage transducers; voltage, with a voltage transducer (electrically isolated); current, with a shunt and transducer; and the air flow rate, with a choked-flow nozzle. The data were stored on magnetic tape at the rate of 400 samples per second.

On the basis of calibrations and data-reduction techniques, the estimated accuracy of the measured data is as follows:

Voltage . . . . .	±3 percent
Pressure . . . . .	±2 percent
Wall heat flux . . . . .	±20 W/cm <sup>2</sup>

### ANALYSIS

#### Mathematical Model

For the purposes of the analysis, the wall-stabilized constricted arc is considered to be a constant-area-pipe flow apparatus; that is, flow is parallel to and symmetric about the tube center line (no swirl flow). No transpiration of gases at the wall is allowed; thus, the mass flow rate is constant. A sketch of the mathematical model of the arc heater showing coordinates and flow direction is given in figure 2.

#### Simplifying Assumptions

In the analysis of the wall-stabilized constricted arc, the following major assumptions are made:

- (1) The flow consists of a real gas that is in local thermodynamic equilibrium.
- (2) The gas is optically transparent to all thermal radiation.
- (3) The flow is steady and axisymmetric; that is, no axial pulsations or tangential variations exist.
- (4) Considered as a whole, the gas is electrically neutral and the electromagnetic effects are negligible.
- (5) The usual velocity and thermal boundary-layer approximations are valid. (See, e.g., ref. 2.)

## Governing Equations

The geometry of the constricted arc is such that the cylindrical coordinate system is a natural choice for the conservation equations. Under the simplifying assumptions given, the Navier-Stokes equations in cylindrical coordinates for the present analysis reduce to:

Continuity,

$$\frac{\partial(\rho u)}{\partial z} + \frac{1}{r} \frac{\partial(\rho v r)}{\partial r} = 0 \quad (1)$$

Momentum,

$$\rho u \frac{\partial u}{\partial z} + \rho v \frac{\partial u}{\partial r} = -\frac{dp}{dz} + \frac{1}{r} \frac{\partial}{\partial r} \left( r \mu \frac{\partial u}{\partial r} \right) \quad (2)$$

Energy,

$$\rho u \frac{\partial H}{\partial z} + \rho v \frac{\partial H}{\partial r} = \frac{1}{r} \frac{\partial}{\partial r} \left\{ r \frac{k}{c_p} \left[ \frac{\partial H}{\partial r} + (N_{Pr} - 1) u \frac{\partial u}{\partial r} \right] \right\} + \gamma E_z^2 - Q \quad (3)$$

where the radiated power  $Q$  is

$$Q = 4\bar{\mu}_p \sigma T^4$$

In addition, Ohm's law and the integral form of the continuity equation (mass-flow equation) will be useful in the numerical solution technique:

$$I = 2\pi E_z \int_0^{r_w} \gamma r \, dr \quad (4)$$

$$2\pi \int_0^{r_w} \rho u r \, dr = \dot{m} \quad (5)$$

In the energy equation (eq. (3)), the Joule heating term  $\gamma E_z^2$  can be simplified by using Ohm's law (eq. (4)) to

$$\gamma E_z^2 = \frac{\gamma I^2}{\left( \int_0^{r_w} 2\pi r \gamma \, dr \right)^2} \quad (6)$$

The following nondimensional variables are introduced:

$$\begin{aligned}
 U &= \frac{u}{u_o} & V &= \frac{v}{u_o} N_{Re,o} & \bar{p} &= \frac{p - p_o}{\rho_o u_o^2} \\
 \bar{H} &= \frac{H}{h_o} & R &= \frac{r}{r_w} & \bar{z} &= \frac{z}{r_w N_{Re,o}} & N_{Re,o} &= \frac{\rho_o u_o 2r_w}{\mu_o} \\
 N_{Pr,o} &= \frac{\mu_o c_{p,o}}{k_o} & \bar{\rho} &= \frac{\rho}{\rho_o} & \bar{\mu} &= \frac{\mu}{\mu_o} \\
 \bar{k} &= \frac{k}{k_o} & \bar{c}_p &= \frac{c_p}{c_{p,o}} & \bar{\gamma} &= \frac{\gamma}{\gamma_o}
 \end{aligned}$$

$$\bar{I} = I \sqrt{\frac{N_{Re,o}}{\rho_o u_o h_o r_w^3 \gamma_o}}$$

$$\bar{Q} = Q \frac{r_w N_{Re,o}}{\rho_o u_o h_o}$$

The reference conditions are calculated from

$$F_o = 2 \int_0^1 F|_{\bar{z}=0} R dR$$

Upon introduction of the nondimensional quantities, the governing equations become:

Continuity,

$$\frac{\partial(\bar{\rho}U)}{\partial\bar{z}} + \frac{1}{R} \frac{\partial(\bar{\rho}VR)}{\partial R} = 0 \tag{7}$$

Momentum,

$$\bar{\rho}U \frac{\partial U}{\partial\bar{z}} + \bar{\rho}V \frac{\partial U}{\partial R} - \frac{2}{R} \frac{\partial}{\partial R} \left( R \bar{\mu} \frac{\partial U}{\partial R} \right) + \frac{d\bar{p}}{d\bar{z}} = 0 \tag{8}$$

Energy,

$$\begin{aligned} \bar{\rho} U \frac{\partial \bar{H}}{\partial \bar{z}} + \bar{\rho} V \frac{\partial \bar{H}}{\partial R} - \frac{1}{N_{Pr,o}} \frac{2}{R} \frac{\partial}{\partial R} \left( R \frac{\bar{k}}{c_p} \frac{\partial \bar{H}}{\partial R} \right) = \frac{1}{N_{Pr,o}} \frac{2u_o^2}{h_o} \frac{1}{R} \frac{\partial}{\partial R} \left[ R \frac{\bar{k}}{c_p} (N_{Pr,o} N_{Pr} - 1) U \frac{\partial U}{\partial R} \right] \\ + \frac{\bar{\gamma} \bar{I}^2}{\left( \int_0^1 2\pi \bar{\gamma} R \, dR \right)^2} - \bar{Q} \end{aligned} \quad (9)$$

The nondimensional form of equation (5) is

$$\int_0^1 \bar{\rho} U R \, dR = \frac{\dot{m}}{2\pi \rho_o u_o r_w^2} \quad (10)$$

#### Boundary Conditions

The boundary conditions on the governing equations are

$$V = 0 \quad \frac{dU}{dR} = 0 \quad \frac{d\bar{H}}{dR} = 0 \quad (\text{at } R = 0)$$

$$V = 0 \quad U = 0 \quad \bar{H} = \bar{H}_w \quad (\text{at } R = 1)$$

#### Turbulent Case

When turbulent flow is considered, the transport terms are defined as follows:

$$\bar{\mu}_e = \bar{\mu} + \frac{\rho_o \bar{\rho} \epsilon_m}{\mu_o}$$

$$\left. \frac{\bar{k}}{c_p} \right|_e = \frac{\bar{k}}{c_p} + \frac{\rho_o c_{p,o} \bar{\rho} \epsilon_m}{k_o N_{Pr,t}}$$

where

$$N_{Pr,t} = \frac{\epsilon_m}{\epsilon_h}$$

The eddy viscosity  $\epsilon_m$  is calculated by the following relations from reference 4:

$$\left. \begin{aligned} \lambda &= 0.4(1 - R) \left\{ 1 - \exp \left[ - \frac{(1 - R) \sqrt{\tau_w / \rho_w}}{26} \right] \right\} \\ \epsilon_m &= \lambda^2 \left| \frac{dU}{dR} \right| \end{aligned} \right\} \quad (11)$$

### Thermophysical Properties

The properties needed for air were assembled from several sources:

Property	Source
$\mu, k, c_p, h, Z$	Reference 5
$\bar{\mu}_P$	Reference 6
$\gamma$	Reference 7

These properties as a function of pressure (or density) and temperature were input into the program.

### NUMERICAL SOLUTIONS

Because of the highly nonlinear character of the governing equations, a numerical solution is dictated.

In the solution scheme, the derivatives in the energy and momentum equations are replaced by their corresponding finite-difference form. (See the appendix.) The momentum equation contains two related unknowns,  $U$  and  $\bar{p}$ ; consequently, another equation is needed (in addition to eq. (8)) to solve for these two unknowns. Equation (10) is the additional relation needed, and the finite-difference form is obtained from Simpson's rule. (See the appendix.) In order to illustrate the solution technique, the finite-difference forms of equations (8) and (10) are developed as follows (see fig. 3 for nodal indexing):

Momentum equation (eq. (8)),

$$\begin{aligned}
& \bar{\rho}U|_{N,K} \frac{U_{N,K} - U_{N,K-1}}{\Delta \bar{z}} + \bar{\rho}V|_{N,K} \frac{\beta U_{N+1,K} - (\beta - 1)U_{N,K} - U_{N-1,K}}{\beta \delta_2 + \delta_1} \\
& - \frac{4}{R_N \delta_2 \left(1 + \frac{\delta_2}{\delta_1}\right)} \left\{ \left[ \frac{R\bar{\mu}|_{N,K} + R\bar{\mu}|_{N+1,K}}{2\delta_2} + \frac{\beta R\bar{\mu}|_{N,K} \left(\frac{\delta_2^2}{\delta_1^2} - 1\right)}{\beta \delta_2 + \delta_1} \right] U_{N+1,K} \right. \\
& - \left. \left[ \frac{\delta_2^2 \left(\frac{R\bar{\mu}|_{N,K} + R\bar{\mu}|_{N-1,K}}{2\delta_1}\right) + \frac{(\beta - 1)R\bar{\mu}|_{N,K} \left(\frac{\delta_2^2}{\delta_1^2} - 1\right)}{\beta \delta_2 + \delta_1} + \frac{R\bar{\mu}|_{N,K} + R\bar{\mu}|_{N+1,K}}{2\delta_1} \right] U_{N,K} \right. \\
& \left. + \left[ \frac{\delta_2^2 \left(\frac{R\bar{\mu}|_{N,K} + R\bar{\mu}|_{N-1,K}}{2\delta_1}\right) - \frac{R\bar{\mu}|_{N,K} \left(\frac{\delta_2^2}{\delta_1^2} - 1\right)}{\beta \delta_2 + \delta_1} \right] U_{N-1,K} \right\} + \frac{\bar{p}_K - \bar{p}_{K-1}}{\Delta \bar{z}} = 0
\end{aligned}$$

where

$$\delta_2 = R_{N+1} - R_N$$

$$\delta_1 = R_N - R_{N-1}$$

$$\beta = \frac{\delta_1^2}{\delta_2^2}$$

$$\Delta \bar{z} = \bar{z}_K - \bar{z}_{K-1}$$

The momentum equation reduces to the desired form of

$$\tilde{A}_N U_{N-1,K} + \tilde{B}_N U_{N,K} + \tilde{C}_N U_{N+1,K} + \tilde{D}_N \bar{p}_K = \tilde{E}_N \quad (12)$$

where

$$\tilde{A}_N = -\frac{\bar{\rho}V|_{N,K}}{\beta\delta_2 + \delta_1} - \frac{4}{R_N\delta_2\left(1 + \frac{\delta_2}{\delta_1}\right)} \left[ \frac{\delta_2^2}{\delta_1^2} \left( \frac{R\bar{\mu}|_{N,K} + R\bar{\mu}|_{N+1,K}}{2\delta_1} \right) - \left( \frac{R\bar{\mu}|_{N,K}}{\beta\delta_2 + \delta_1} \right) \left( \frac{\delta_2^2}{\delta_1^2} - 1 \right) \right]$$

$$\begin{aligned} \tilde{B}_N = & -\frac{(\beta - 1)\bar{\rho}V|_{N,K}}{\beta\delta_2 + \delta_1} + \frac{\bar{\rho}U_{N,K}}{\Delta\bar{z}} - \frac{4}{R_N\delta_2\left(1 + \frac{\delta_2}{\delta_1}\right)} \left[ \frac{\delta_2^2}{\delta_1^2} \left( \frac{R\bar{\mu}|_{N,K} + R\bar{\mu}|_{N-1,K}}{2\delta_1} \right) \right. \\ & \left. + \frac{(\beta - 1)R\bar{\mu}|_{N,K}}{\beta\delta_2 + \delta_1} \left( \frac{\delta_2^2}{\delta_1^2} - 1 \right) + \frac{R\bar{\mu}|_{N,K} + R\bar{\mu}|_{N+1,K}}{2\delta_1} \right] \end{aligned}$$

$$\tilde{C}_N = \frac{\beta\bar{\rho}V|_{N,K}}{\beta\delta_2 + \delta_1} - \frac{4}{R_N\delta_2\left(1 + \frac{\delta_2}{\delta_1}\right)} \left[ \frac{R\bar{\mu}|_{N,K} + R\bar{\mu}|_{N+1,K}}{2\delta_2} + \frac{\beta R\bar{\mu}|_{N,K}}{\beta\delta_2 + \delta_1} \left( \frac{\delta_2^2}{\delta_1^2} - 1 \right) \right]$$

$$\tilde{D} = \frac{1}{\Delta\bar{z}}$$

$$\tilde{E}_N = \frac{\bar{p}_{K-1} + \bar{\rho}U|_{N,K}U_{N,K-1}}{\Delta\bar{z}}$$

The following form results from the application of Simpson's rule:

Mass-flow equation (eq. (10)),

$$\begin{aligned} \int_0^1 \bar{\rho}UR \, dR &= \tilde{G}_2U_{2,K} + \tilde{H}_3U_{3,K} + \tilde{G}_4U_{4,K} + \tilde{H}_5U_{5,K} + \dots \\ &+ \tilde{G}_N U_{N,K} + \tilde{H}_{N+1} U_{N+1,K} + \tilde{G}_{M-1} \tilde{U}_{M-1,K} \\ &= \tilde{I} \end{aligned} \tag{13}$$

where

$$\tilde{G}_N = \bar{\rho} R|_{N,K} \left[ \frac{(\delta_N + \delta_{N-1})^2}{2\delta_{N-1}} - \frac{(\delta_N + \delta_{N-1})^2}{\delta_N \delta_{N-1}} \left( \frac{\delta_N + \delta_{N-1}}{3} - \frac{\delta_{N-1}}{2} \right) \right]$$

$$\tilde{H}_N = \bar{\rho} R|_{N,K} \left\{ \left( \frac{\delta_{N-1} + \delta_{N-2}}{\delta_{N-1}} \right) \left( \frac{\delta_{N-1} + \delta_{N-2}}{3} - \frac{\delta_{N-2}}{2} \right) + \delta_N + \delta_{N+1} \right.$$

$$\left. - \left[ (\delta_N + \delta_{N+1}) \left( \frac{\delta_N + \delta_{N+1}}{2\delta_N} \right) \left( \frac{\delta_N + \delta_{N+1}}{\delta_N} \right) \left( \frac{\delta_N + \delta_{N+1}}{3} - \frac{\delta_N}{2} \right) \right] \right\}$$

where

$$\delta_{N-2} = R_{N-1} - R_{N-2}$$

$$\delta_{N-1} = R_N - R_{N-1}$$

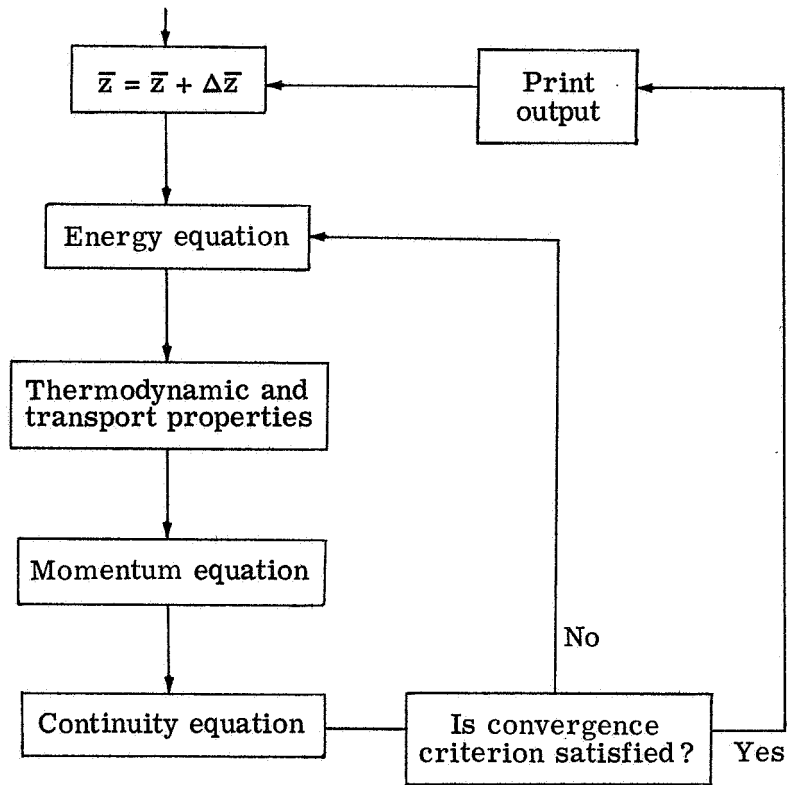
$$\delta_N = R_{N+1} - R_N$$

$$\delta_{N+1} = R_{N+2} - R_{N+1}$$

$$\tilde{I} = \frac{\dot{m}}{2\pi\rho_o u_o r_w^2}$$

Equation (12) is written at each radial grid point (the grid network will be explained in a subsequent section), and equation (13) is added to obtain a set of simultaneous algebraic equations for the unknowns  $U_N$  and  $\bar{p}$ . Additional information on this technique can be found in references 2, 8, and 9. The matrix of coefficients of these equations appears as





#### Nodal Grid

The nodal spacing in the r-direction, from the wall inward to the center line, is taken to be a geometric progression of the form:

$$r_1 = 0$$

$$r_2 = (r_1 + \Delta r)C_r$$

$$r_3 = (r_2 + \Delta r)C_r$$

$$r_i = (r_{i-1} + \Delta r)C_r$$

where  $C_r$  is a constant usually lying between 1.0 and 1.1. The constant  $\Delta r$  is calculated from

$$\Delta r = \frac{C_r - 1}{C_r(C_r^{M-1} - 1)}$$

This particular nodal spacing allows a large number of nodal points to be spaced close to the tube wall, where large changes in the variables take place. Also the axial spacing can be uneven, as shown in figure 3.

### Initial Profiles

In reference 2, it was shown that the shapes of the initial profiles, at  $\bar{z} = 0$ , have little effect on the solutions at short distances downstream; however, in the present study, it was found that it was necessary to give a reasonable estimate for the initial center-line enthalpy  $H_{\zeta}$ , or the effect of the initial profile would persist for some distance down the tube. In the present analysis, the following starting conditions are used:

Enthalpy,

$$H = H_w + (H_{\zeta} - H_w)(1.0 - 3R^2 + 2R^3)$$

Axial velocity,

$$U = U_{\zeta}(1.0 - R^2)$$

(where  $U_{\zeta}$  is obtained from mass-flow constraints)

Radial velocity,

$$V = 0$$

## RESULTS AND DISCUSSION

### Comparisons With Simple Pipe Flows

The present numerical technique has been compared with several simplified solutions from the literature.

Case 1: incompressible entrance flow for a circular pipe, reference 10.- The present solution for laminar incompressible entrance flow and the solution of reference 10 are shown in figure 4 for pressure and in figure 5 for velocity. The agreement is excellent.

Case 2: incompressible laminar-flow heat transfer in the entrance region of a circular pipe, reference 11.- The Nusselt numbers from the present solution and from the solution of reference 11 are shown in figure 6, and the solutions compare favorably.

Case 3: compressible pipe flow with heat transfer, reference 8.- Figure 7 shows the temperature profile for the present solution compared with that of reference 8. Again the agreement is good. An additional comparison of Nusselt numbers and ratios of wall temperature to mean temperature is given in table I for two nondimensional wall temperatures. The agreement is also excellent.

### Comparison With Arc-Heater Experimental Data

Experimental data were taken at two different air flow rates, 2.2 and 4.8 g/sec, and at three different arc-current levels for each flow rate. The results of these measurements are shown in figures 8 and 9 along with the corresponding computed results. The parameters shown in these figures are static pressure, arc voltage, and heat flux to the constrictor wall, all as a function of distance from the upstream end of the arc heater. For an air flow rate of 2.2 g/sec, the numerical calculations closely predict the trends and values for all three parameters. For the air flow rate of 4.8 g/sec, the trends are again well predicted although the values of pressure and voltage near the downstream end are not in quite as close agreement with experiment as are the results for a flow rate of 2.2 g/sec.

In this investigation the operating current and pressure were purposely kept at low values in order to avoid rapid oxidation and destruction of the tungsten cathode. The values of current were less than 600 amperes and the stagnation pressure did not exceed 0.5 atm. According to reference 2, the electromagnetic effects are small as long as the current does not greatly exceed approximately 1000 amperes. At currents much higher than this, the electromagnetic effects may become significant and would be included in the governing equations.

Likewise, the assumption of an optically thin gas is apparently valid at these pressure levels. However, at much higher pressures the validity of this assumption should be examined and appropriate modifications made.

For one case ( $I = 377$  amperes,  $p_0 = 0.40$  atm,  $\dot{m} = 4.8$  g/sec), a radial temperature profile was measured at the axial station  $z = 16$  cm. The temperature profile was determined spectroscopically by the method reported in reference 12 with the use of the 4915 Å NI line. The calculated and the measured profiles are shown in figure 10. The measurement and the calculations both indicate a center-line temperature of about 12 000 K, and there is excellent agreement between the measured and the calculated profile over about 55 percent of the radius. The large difference between the experimental and calculated temperature values near the wall probably results from the experimental setup, primarily the recessing of the quartz window. (See ref. 12 for a discussion of the experimental procedures.) The calculated temperature profile exhibits two marked changes in slope corresponding to regions of rapid variation in two thermophysical properties. The first rapid change is in the temperature range 2500 K to 3500 K, which corresponds to a region of rapid variation in the thermal conductivity. The second change is in the temperature range 5000 K to 7000 K, which corresponds to the region of rapid rise in electrical conductivity. Thus, what appear as oscillations in the solution are really thermophysical property effects.

## CONCLUDING REMARKS

Within the range of investigation the implicit, iterative numerical technique developed herein for the analysis of the wall-stabilized constricted arc was shown to describe adequately the fluid mechanic, thermal, and electrical variables. The range investigated included arc currents from 377 to 584 amperes and a gas entrance pressure of approximately 0.40 atm with gas flow rates of 2.2 and 4.8 g/sec. Predictions for operation at much higher pressures (several atmospheres) may require further examination of the assumption that the gas is optically transparent. Also, much higher currents and very low pressures may necessitate the inclusion of electromagnetic effects in the governing equations in order to maintain the degree of accuracy exhibited in this study.

Langley Research Center,  
National Aeronautics and Space Administration,  
Hampton, Va., December 15, 1972.

## APPENDIX

### FINITE-DIFFERENCE RELATIONS

The following finite-difference relations are used to reduce the governing differential equations to difference equations:

First-order axial derivatives,

$$\left. \frac{\partial f}{\partial \bar{z}} \right|_{N,K} = \frac{f_{N,K} - f_{N,K-1}}{\Delta \bar{z}}$$

First-order radial derivatives (unequal spacing),

$$\left. \frac{\partial f}{\partial R} \right|_{N,K} = \frac{\beta f_{N+1,K} - (\beta - 1)f_{N,K} - f_{N-1,K}}{\beta \delta_2 + \delta_1}$$

where

$$\beta = \frac{\delta_1^2}{\delta_2^2}$$

$$\delta_1 = R_N - R_{N-1}$$

$$\delta_2 = R_{N+1} - R_N$$

Second-order radial derivatives (unequal spacing),

$$\begin{aligned} \left. \frac{\partial}{\partial R} \left( F \frac{\partial f}{\partial R} \right) \right|_{N,K} &= \frac{2}{\delta_2 \left( 1 + \frac{\delta_2}{\delta_1} \right)} \left\{ \frac{F_N + F_{N+1}}{2} \left( \frac{f_{N+1,K} - f_{N,K}}{\delta_2} \right) + F_N \left( \frac{\delta_2^2}{\delta_1^2} - 1 \right) \right. \\ &\quad \left. \times \left[ \frac{\beta f_{N+1,K} - (\beta - 1)f_{N,K} - f_{N-1,K}}{\beta \delta_2 + \delta_1} \right] - \frac{1}{\beta} \frac{F_N + F_{N-1}}{2} \left( \frac{f_{N,K} - f_{N-1,K}}{\delta_1} \right) \right\} \end{aligned}$$

APPENDIX – Concluded

Three-point unevenly spaced integration formula (Simpson's rule),

$$\begin{array}{ccc} & \delta_1 & \delta_2 \\ \overset{0}{1} & & \overset{0}{2} & & \overset{0}{3} \end{array}$$

$$\int_{r_1}^{r_3} f(r) dr = \left[ \frac{\delta_1 + \delta_2}{2} \left( 1 - \frac{\delta_1 + \delta_2}{3\delta_1} \right) \right] f_1 + \left[ \frac{(\delta_1 + \delta_2)^2}{\delta_1} \left( \frac{1}{2} - \frac{\delta_1 + \delta_2}{3\delta_2} + \frac{\delta_1}{2\delta_2} \right) \right] f_2$$

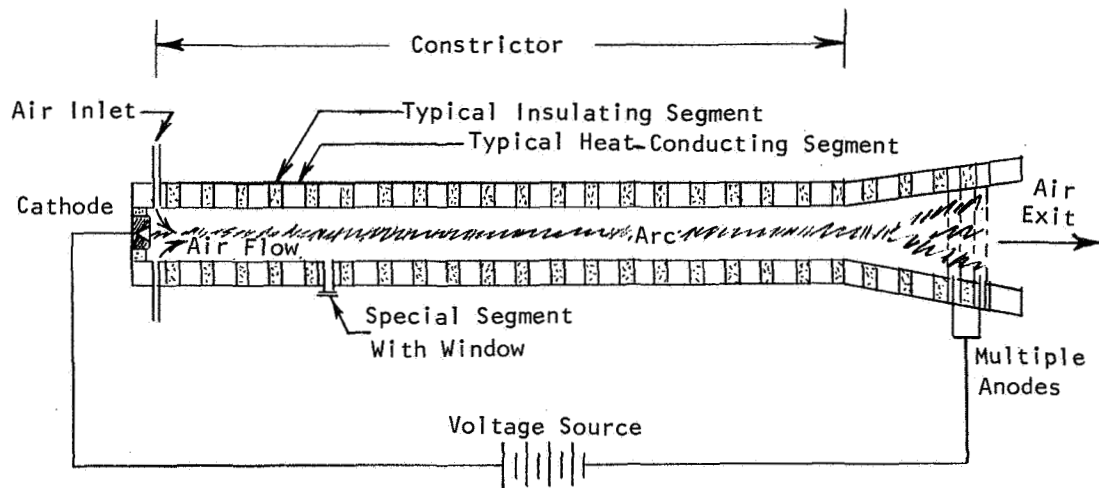
$$+ \left[ \frac{(\delta_1 + \delta_2)^2}{3\delta_2} - \frac{\delta_1}{\delta_2} \frac{\delta_1 + \delta_2}{2} \right] f_3$$

## REFERENCES

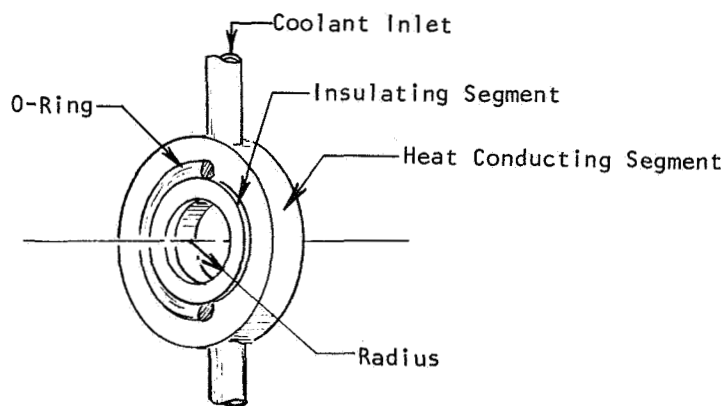
1. Skifstad, James G.: Review of Theoretical Analyses of Arc Heating in a Tube. ARL 65-207, U.S. Air Force, Oct. 1965. (Available from DDC as AD 625 558.)
2. Bower, William Walter: Correlations for the Wall Parameters in the Asymptotic Region of a Laminar Constricted Arc. M.S. Thesis, Purdue Univ., Jan. 1969.
3. Watson, Velvin R.; and Pegot, Eva B.: Numerical Calculations for the Characteristics of a Gas Flowing Axially Through a Constricted Arc. NASA TN D-4042, 1967.
4. Bankston, C. A.; and McEligot, D. M.: Turbulent and Laminar Heat Transfer to Gases With Varying Properties in the Entry Region of Circular Ducts. Int. J. Heat & Mass Transfer, vol. 13, no. 2, Feb. 1970, pp. 319-344.
5. Hansen, C. Frederick: Approximations for the Thermodynamic and Transport Properties of High-Temperature Air. NASA TR R-50, 1959. (Supersedes NACA TN 4150.)
6. Landshoff, Rolf K. M.; and Magee, John L.: Thermal Radiation Phenomena. Vol. 1 - Radiative Properties of Air. IFI/Plenum Data Corp., 1969.
7. Arave, R. J.: The Thermodynamic Properties of Air in Dissociation and Ionization Equilibrium From 500 °K to 25,000 °K. Doc. No. D2-9909, Boeing Company, 1961. (Available from DDC as AD 438 260.)
8. Worsøe-Schmidt, P. M.; and Leppert, G.: Heat Transfer and Friction for Laminar Flow of Gas in a Circular Tube at High Heating Rate. Int. J. Heat & Mass Transfer, vol. 8, no. 10, Oct. 1965, pp. 1281-1301.
9. Hwang, Ching-Lai; and Fan, Liang-Tseng: A Finite Difference Analysis of Laminar Magneto-Hydrodynamic Flow in the Entrance Region of a Flat Rectangular Duct. Appl. Sci. Res., Sec. B, vol. 10, no. 3-4, 1963, pp. 329-343.
10. Hornbeck, Robert W.: Laminar Flow in the Entrance Region of a Pipe. Appl. Sci. Res., sec. A, vol. 13, 1964, pp. 224-232.
11. Manohar, R.: Analysis of Laminar-Flow Heat Transfer in the Entrance Region of Circular Tubes. Int. J. Heat & Mass Transfer, vol. 12, no. 1, Jan. 1969, pp. 15-22.
12. Snow, Walter L.: Practical Consideration for Abel Inverting of Photographic Data With Application to the Analysis of a 15-kW Wall-Stabilized Arc-Light Source. NASA TN D-6672, 1972.

TABLE I.- NUSSELT NUMBERS AND RATIOS OF WALL TEMPERATURE TO MEAN TEMPERATURE FOR COMPRESSIBLE PIPE FLOW WITH HEAT TRANSFER

$\bar{z}$	$N_{Nu}$		$T_w/T_m$	
	Present	Reference 8	Present	Reference 8
$\theta_w = 0.5$				
0.001	12.02	11.98	0.508	0.508
.002	9.41	9.41	.514	.514
.005	6.95	6.90	.525	.525
.01	5.63	5.62	.540	.540
.02	4.68	4.69	.564	.564
.05	3.94	3.94	.619	.619
.1	3.74	3.71	.695	.692
$\theta_w = 2.0$				
0.001	14.46	14.62	1.92	1.92
.002	11.25	11.31	1.87	1.87
.005	8.11	8.04	1.78	1.78
.01	6.34	6.30	1.68	1.69
.02	5.03	5.00	1.57	1.56
.05	3.95	3.92	1.37	1.36
.1	3.65	3.62	1.19	1.19



(a) Schematic of constricted-arc heater.



(b) Typical section of constrictor.

Figure 1.- Schematic of arc heater used for experimental measurements.

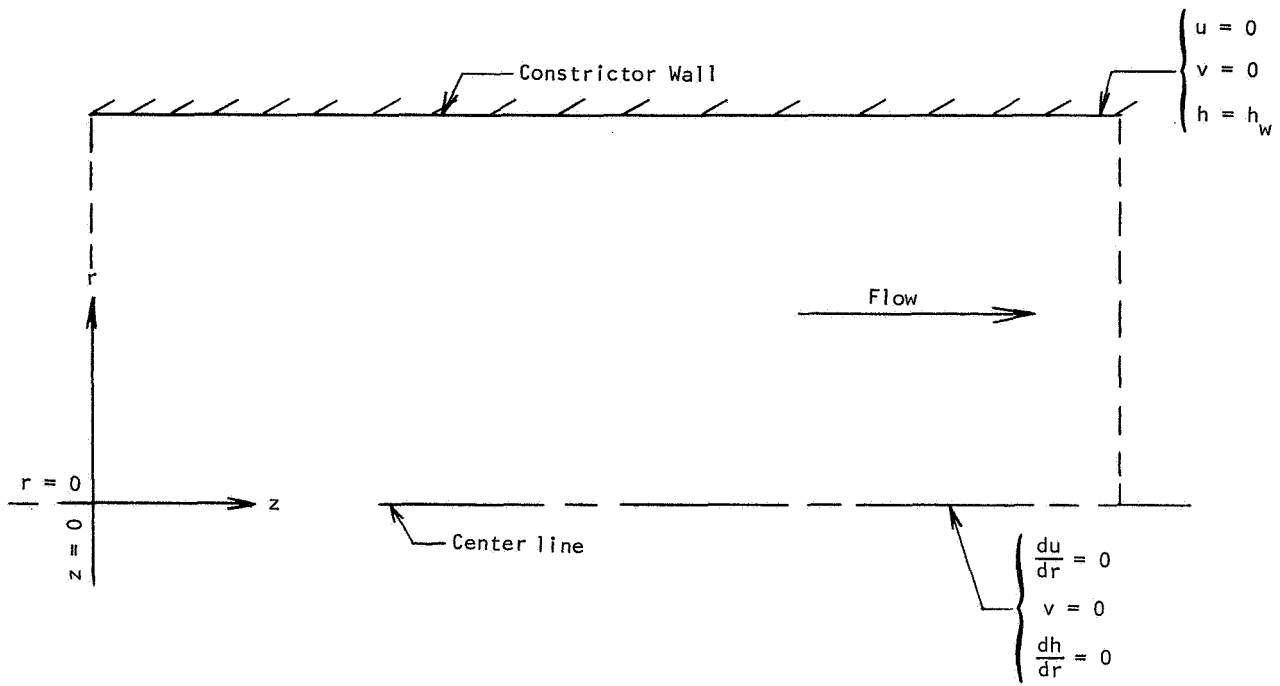


Figure 2.- Sketch of mathematical model of arc heater.

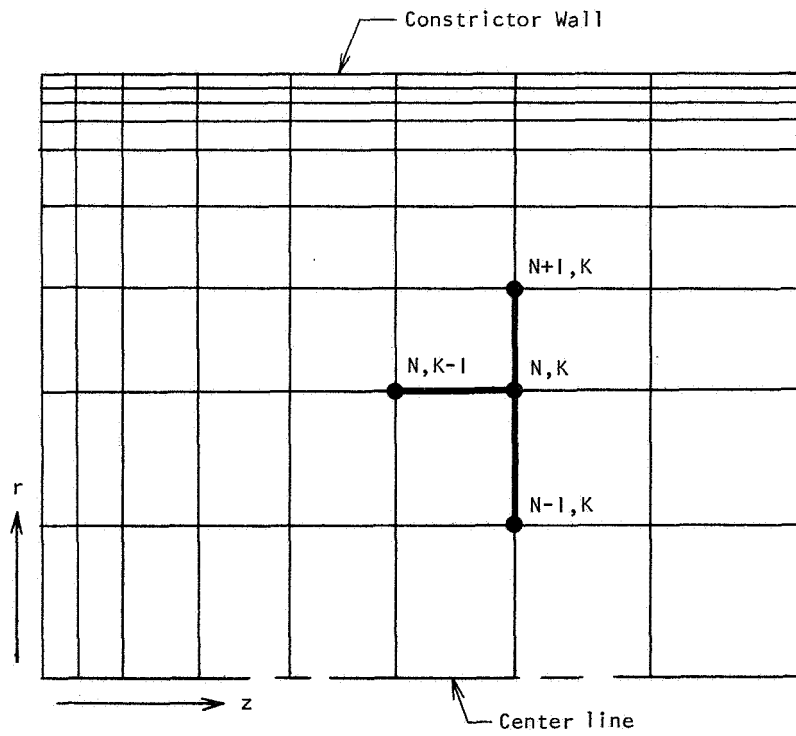


Figure 3.- Representation of nodal spacing used in numerical calculations.

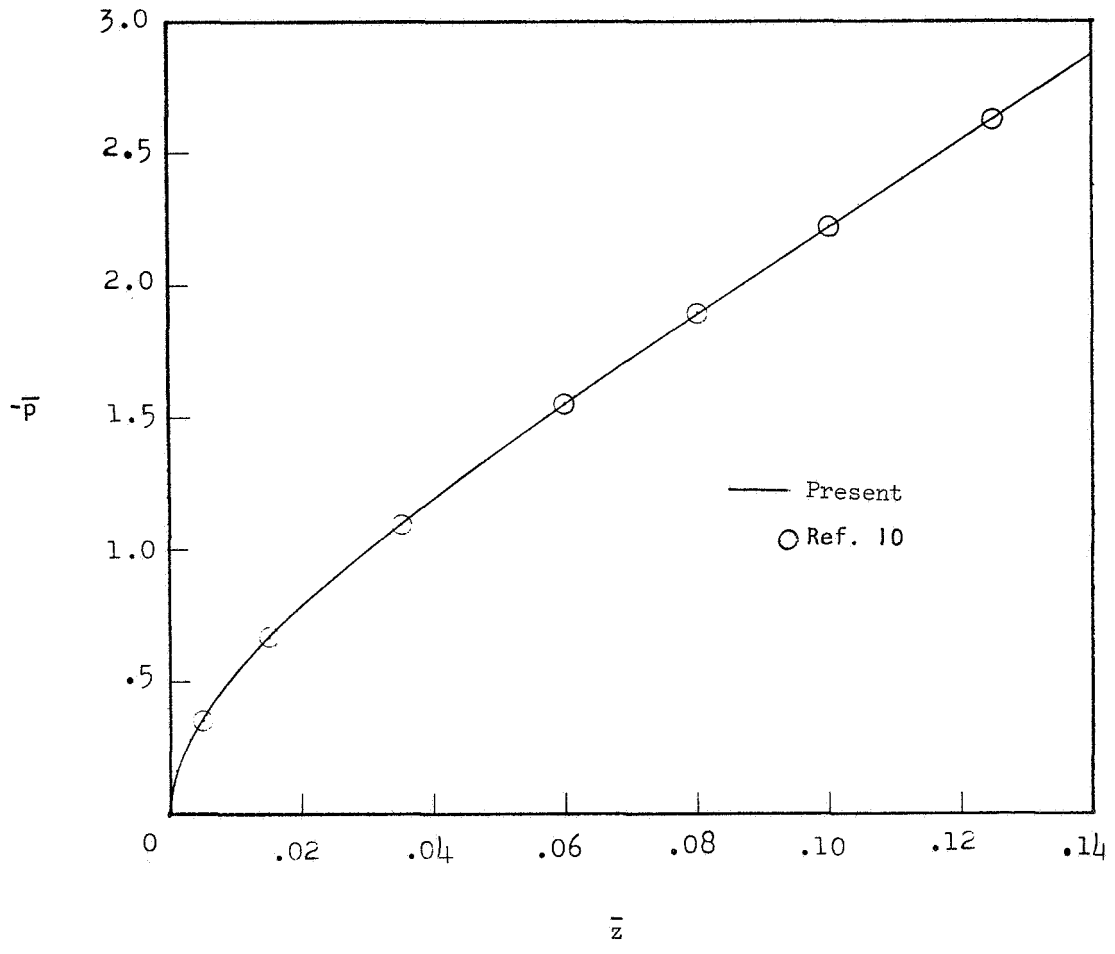


Figure 4.- Comparison of pressure from present numerical calculations and that of reference 10 for laminar incompressible entrance flow in a circular pipe.

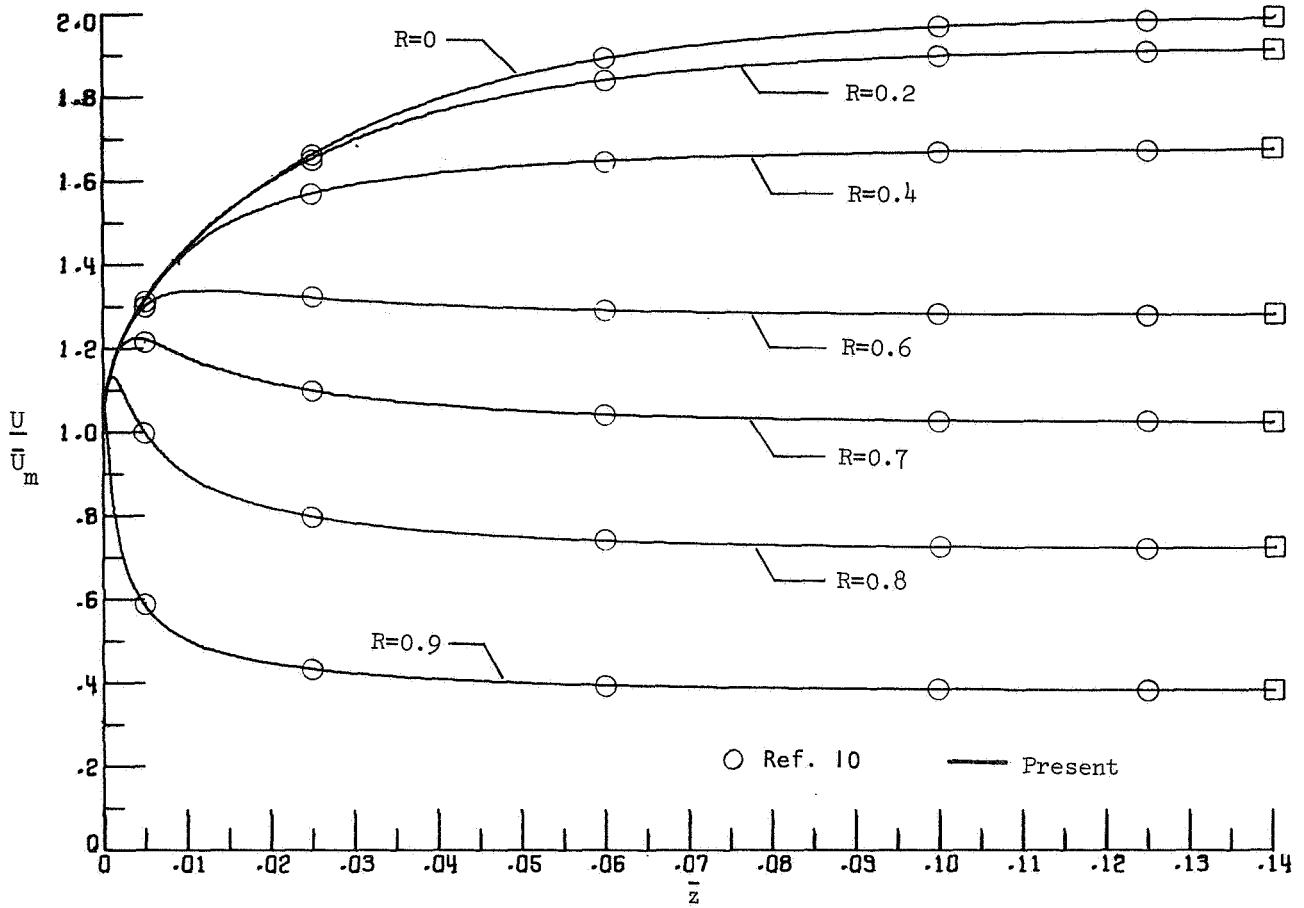


Figure 5.- Comparison of velocity from present numerical calculations and from reference 10 for laminar incompressible entrance flow in a circular pipe. (Square symbols indicate fully developed pipe flow.)

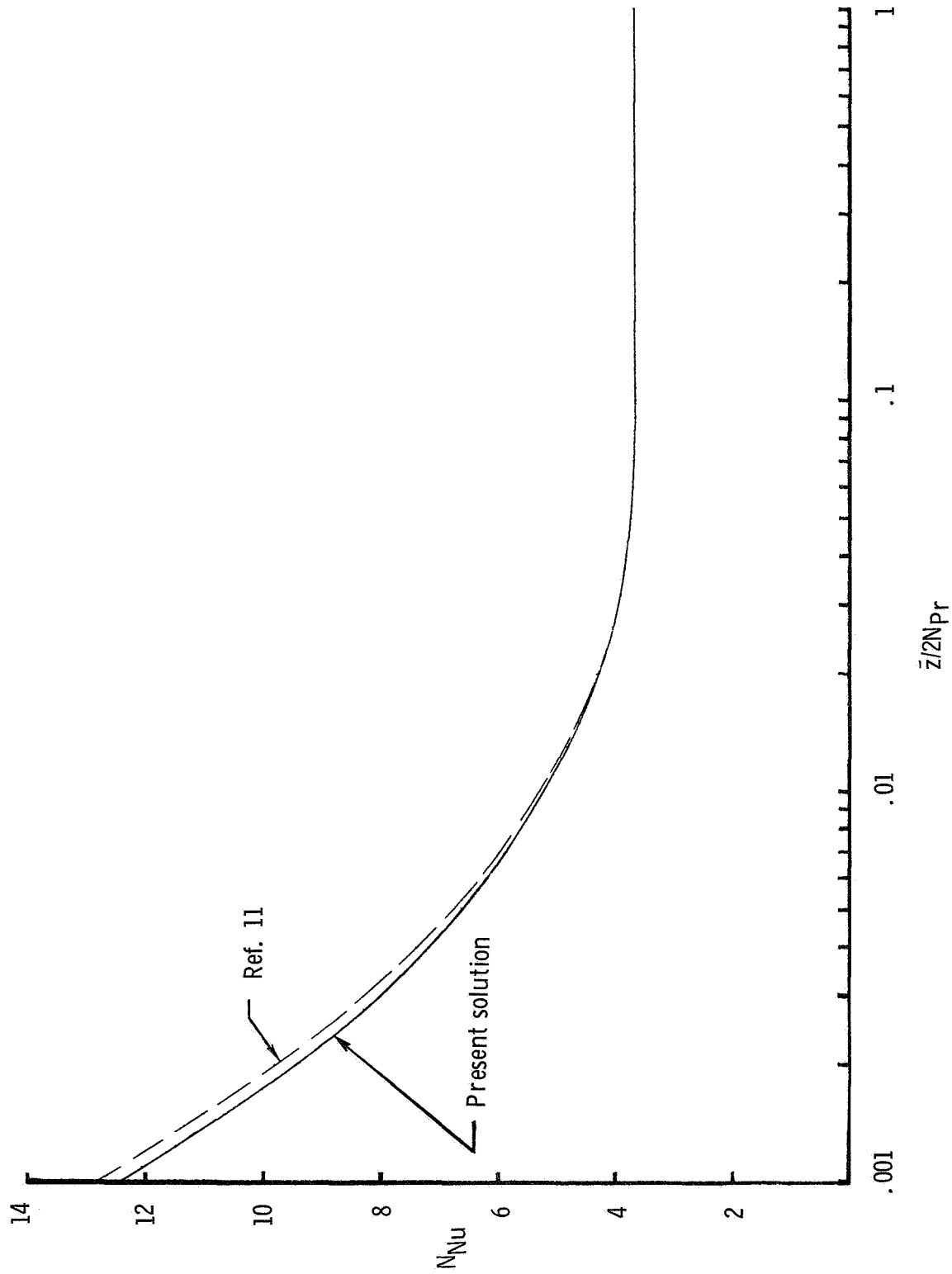


Figure 6.- Comparison of Nusselt number from present numerical calculations and from that of reference 11 for incompressible laminar entrance flow in a circular pipe.  $N_{Pr} = 0.70$ .

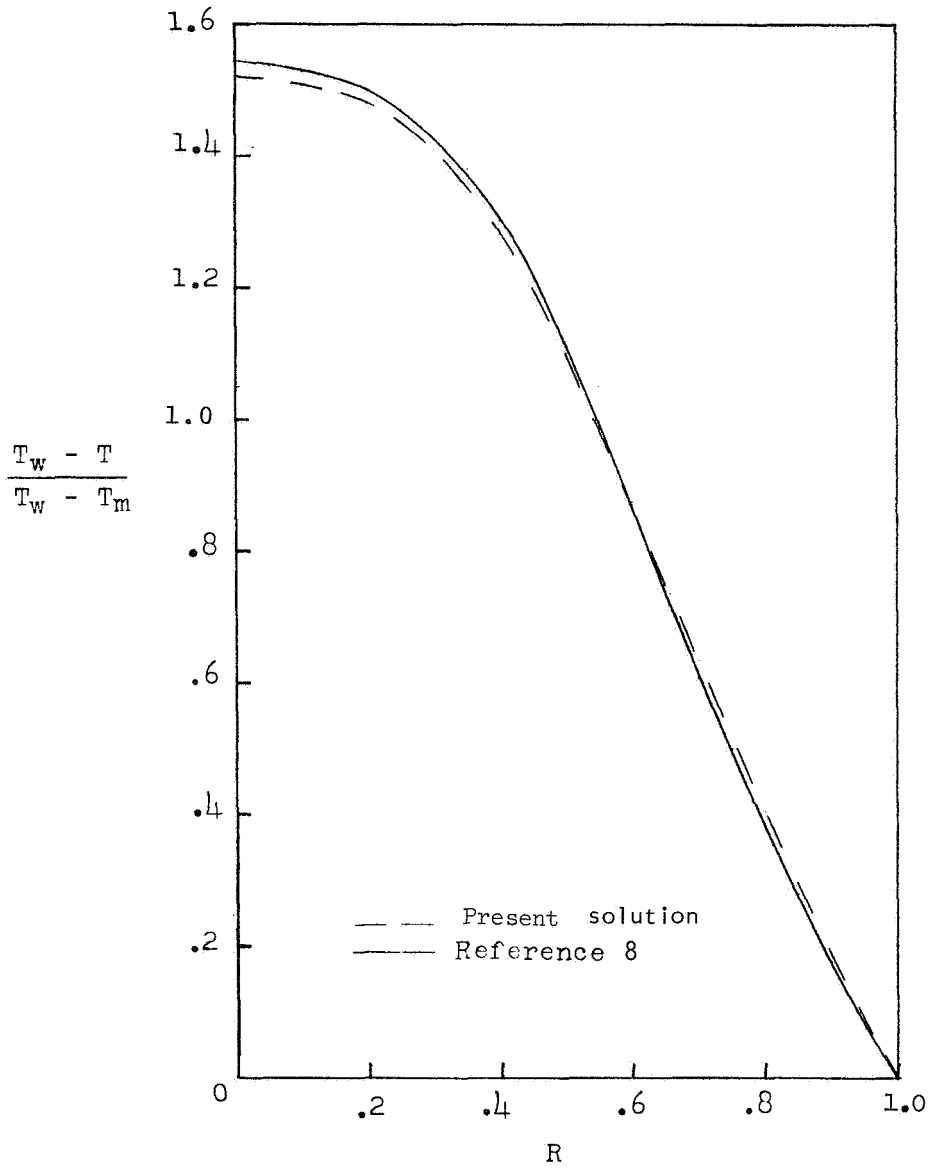
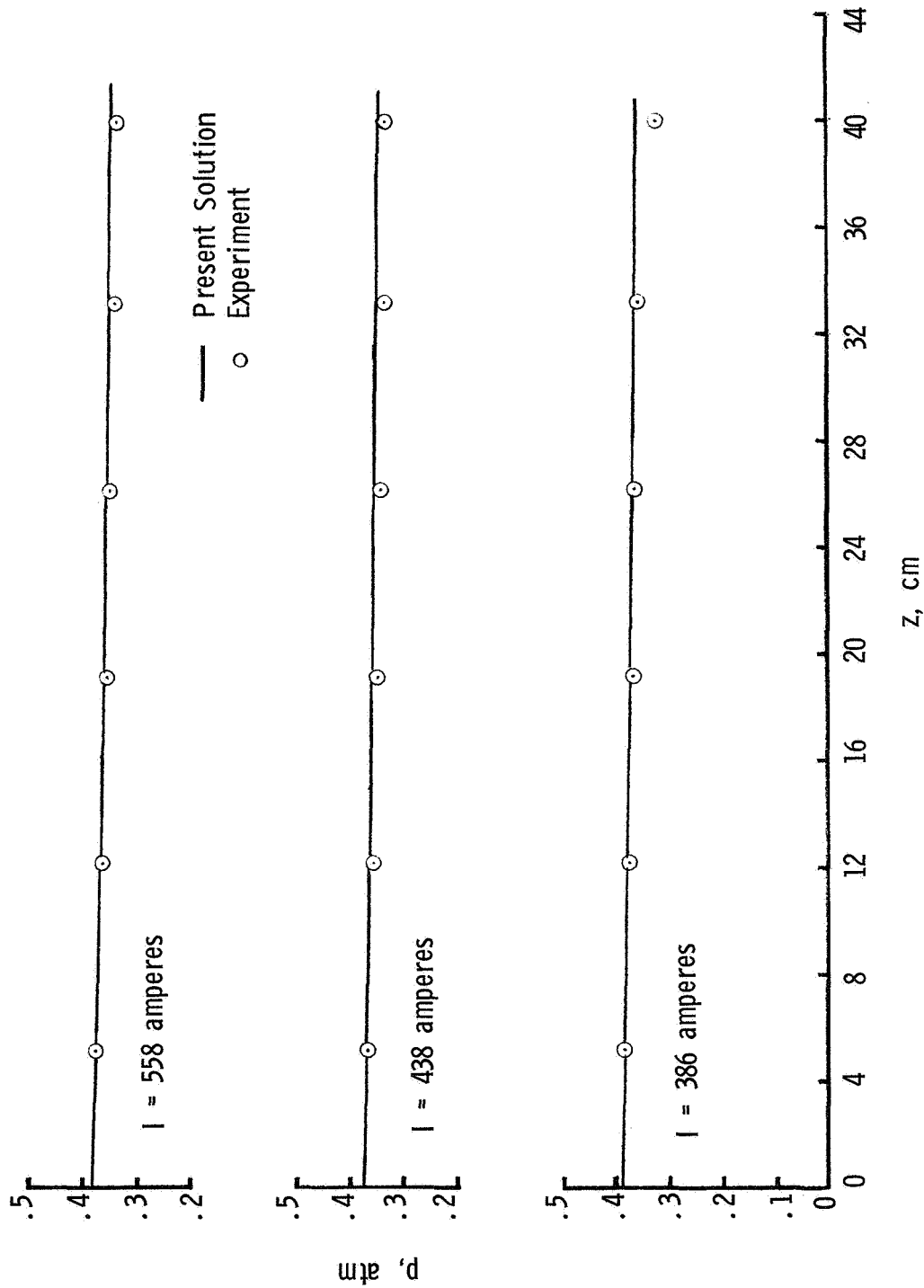
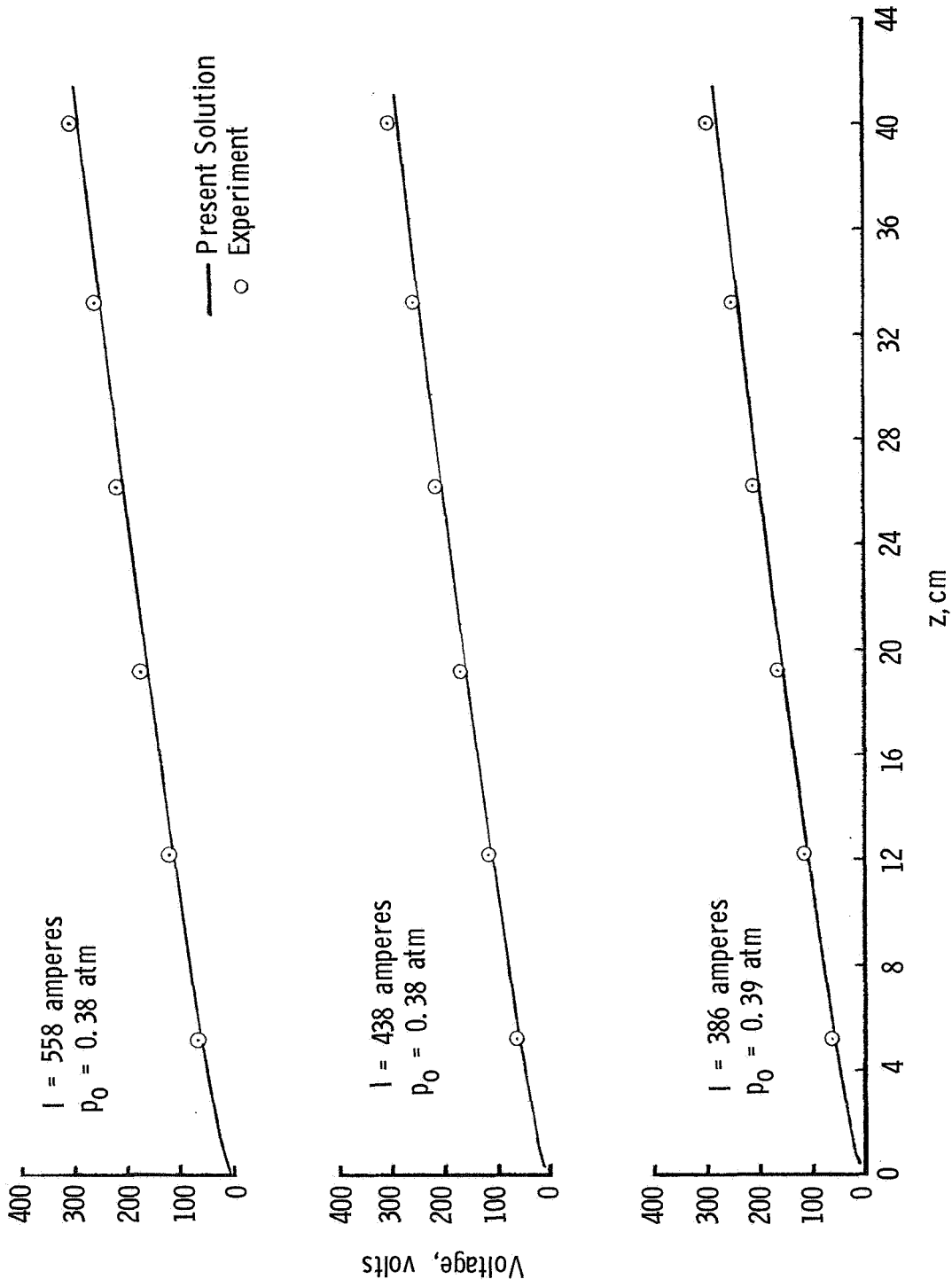


Figure 7.- Comparison of temperature profile at  $\bar{z} = 0.03$  from present numerical calculations and that of reference 8 for compressible pipe flow with heat transfer.



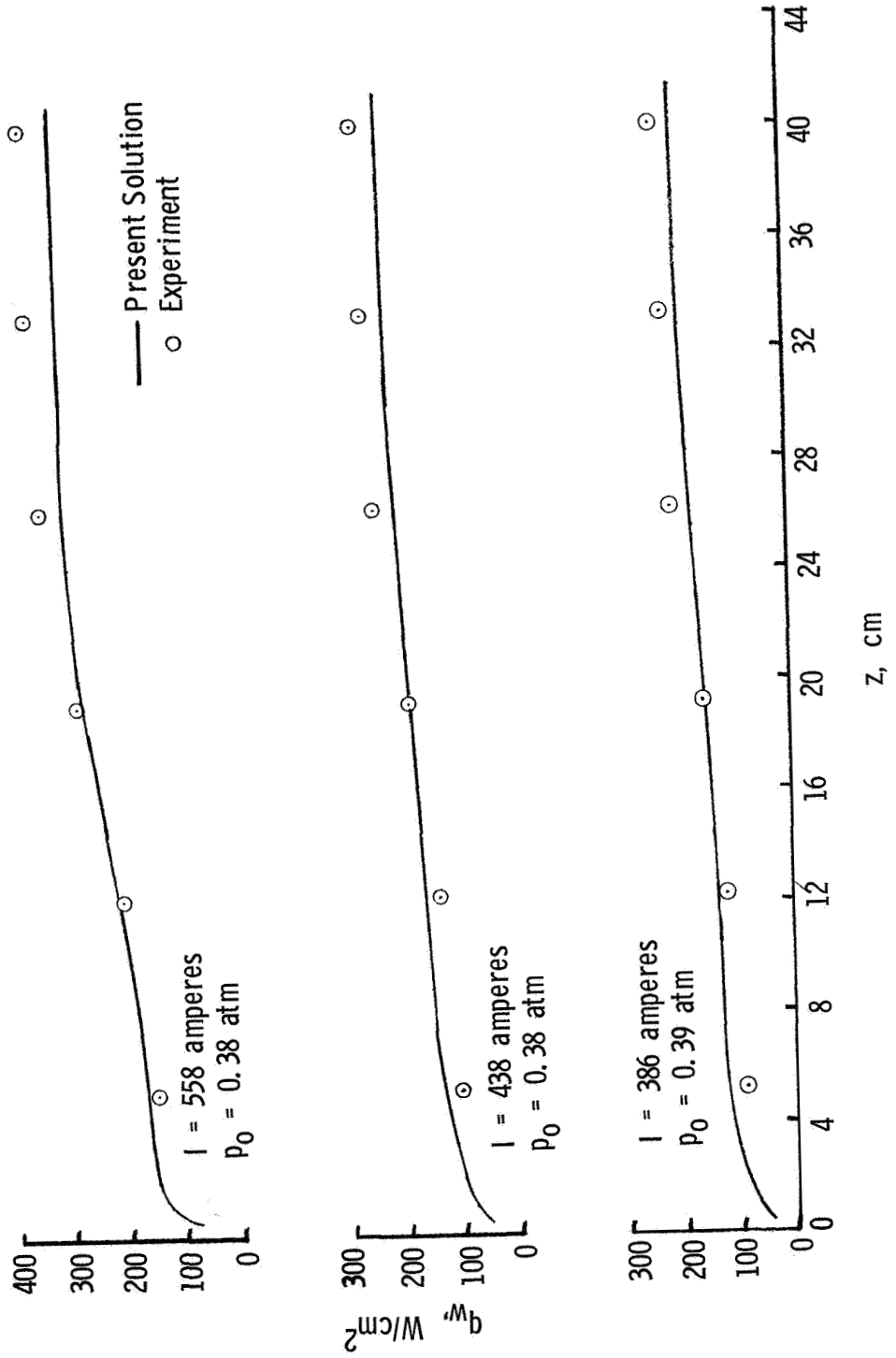
(a) Static pressure.

Figure 8.- Comparison of arc-heater experimental data with numerical solutions for  $\dot{m} = 2.2$  g/sec.



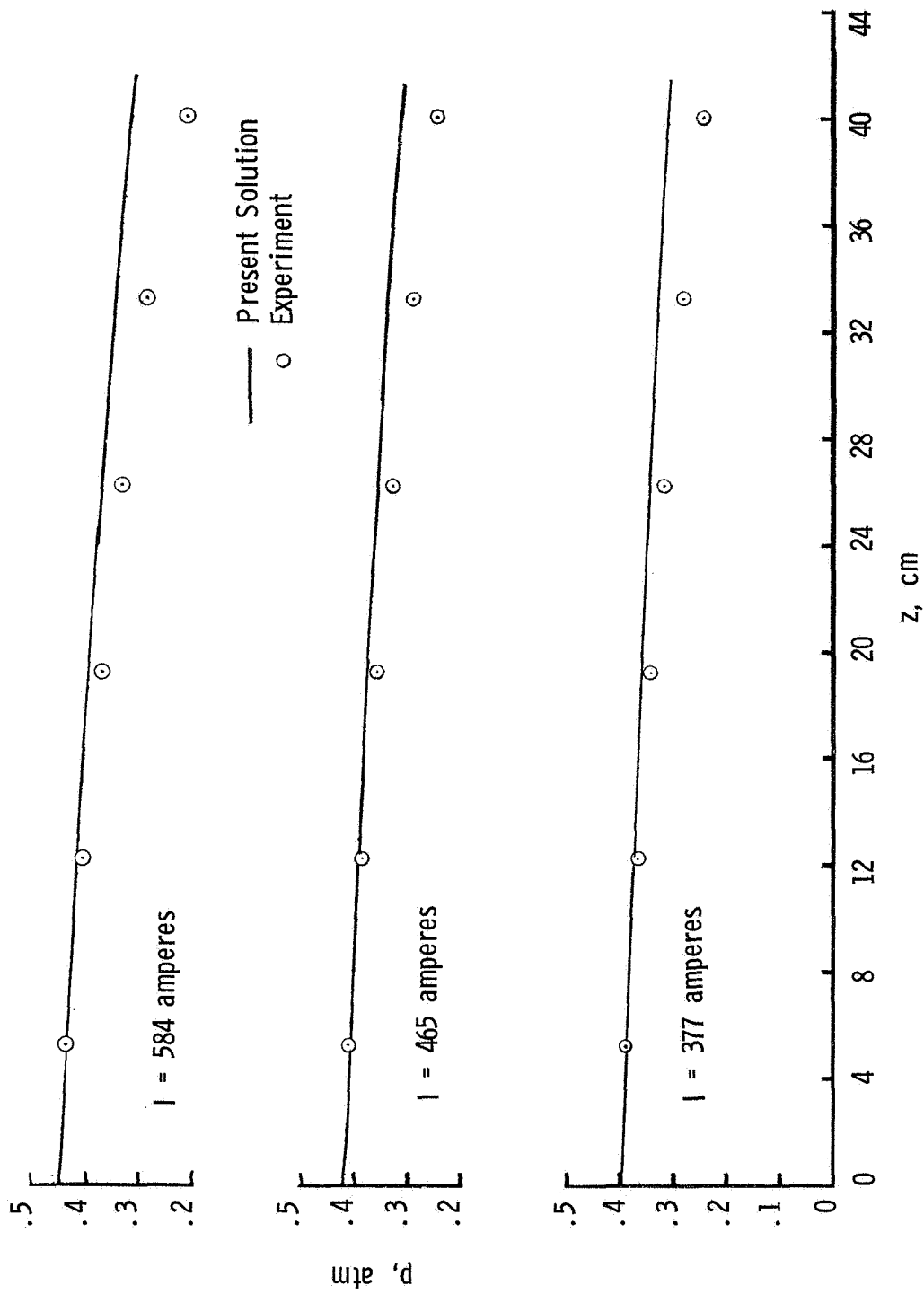
(b) Voltage, referenced to the cathode.

Figure 8.- Continued.



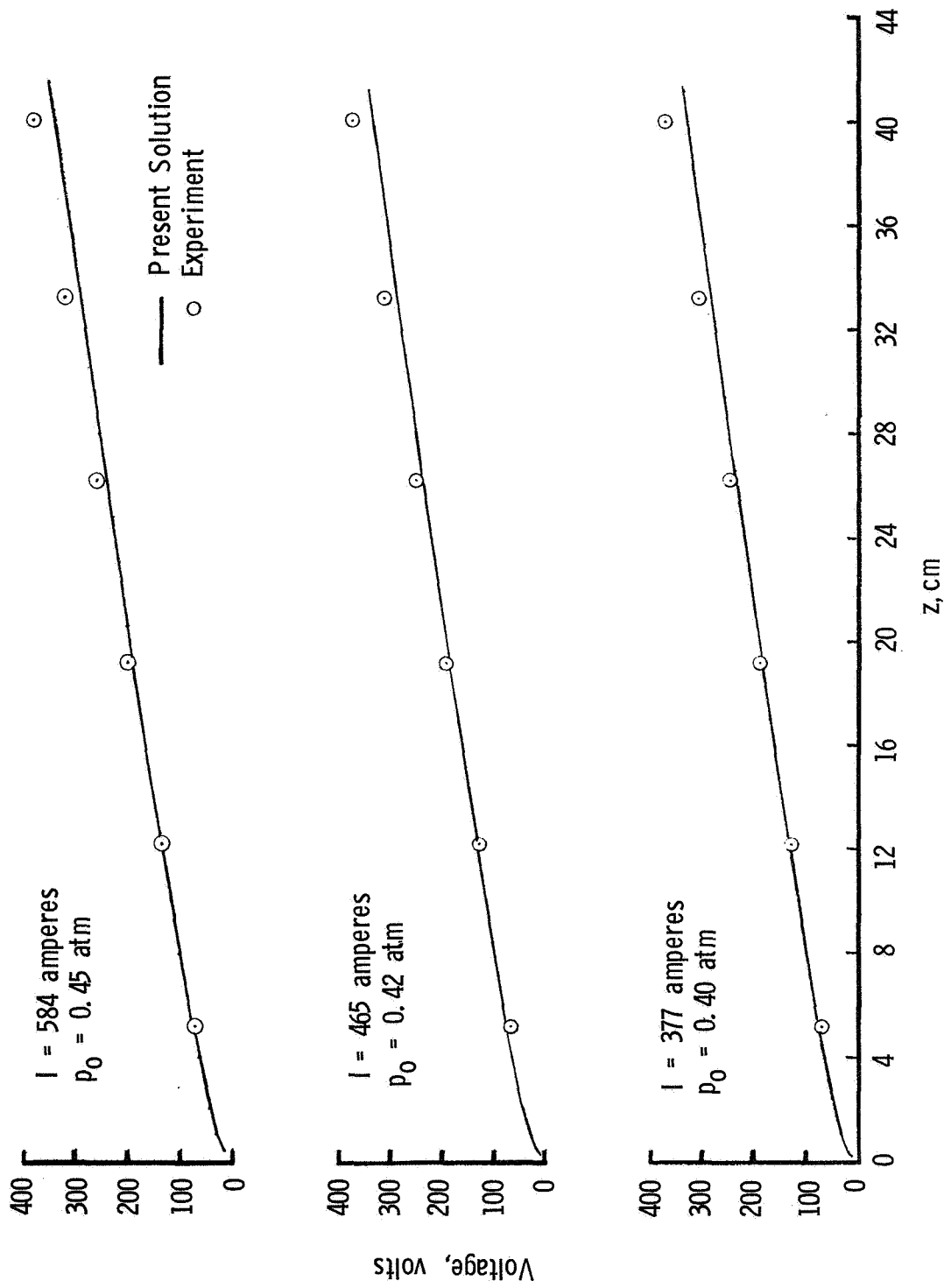
(c) Wall heat flux.

Figure 8.- Concluded.



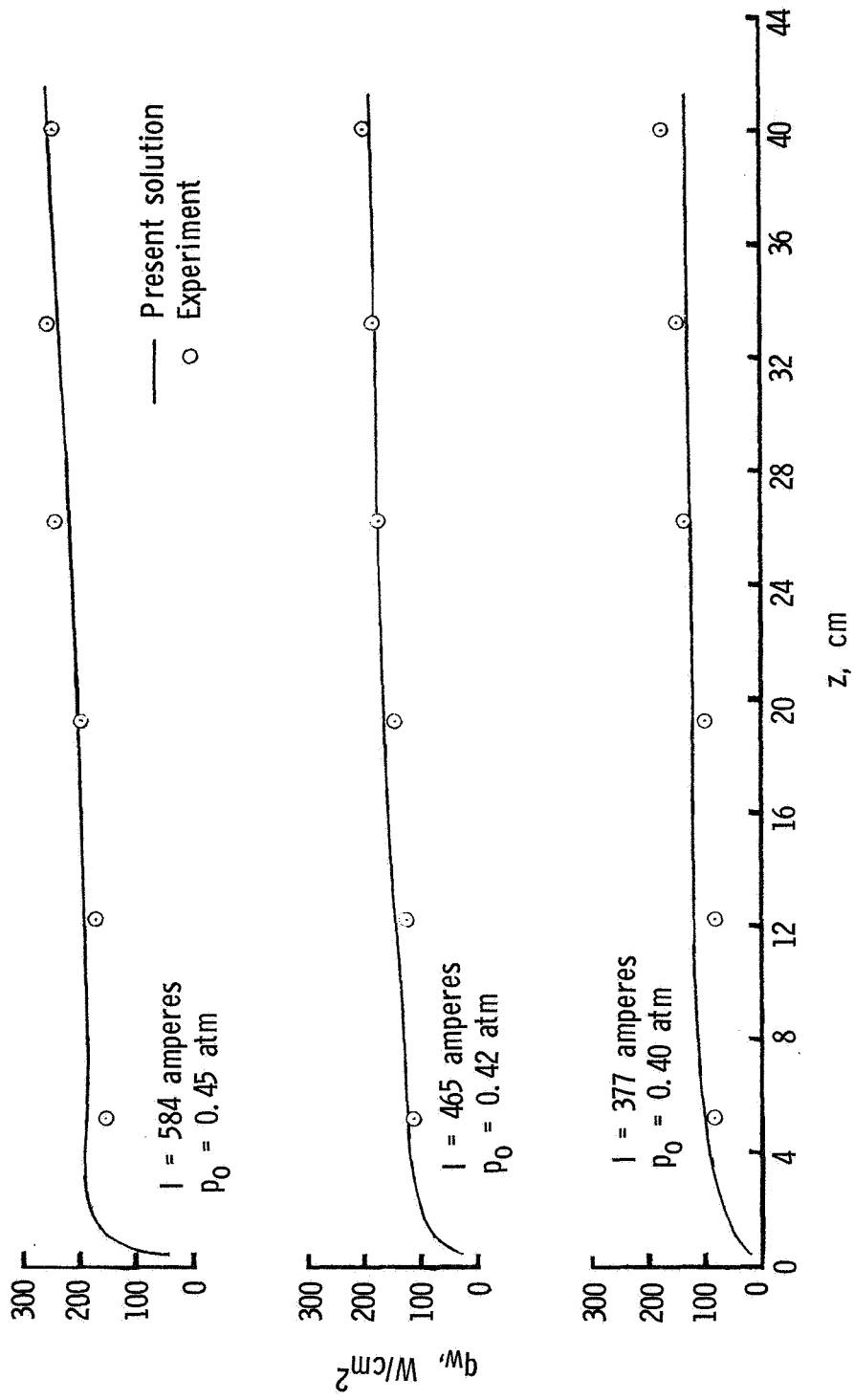
(a) Static pressure.

Figure 9.- Comparison of arc-heater experimental data with numerical solutions for  $\dot{m} = 4.8$  g/sec.



(b) Voltage, referenced to the cathode.

Figure 9.- Continued.



(c) Wall heat flux.  
Figure 9.- Concluded.

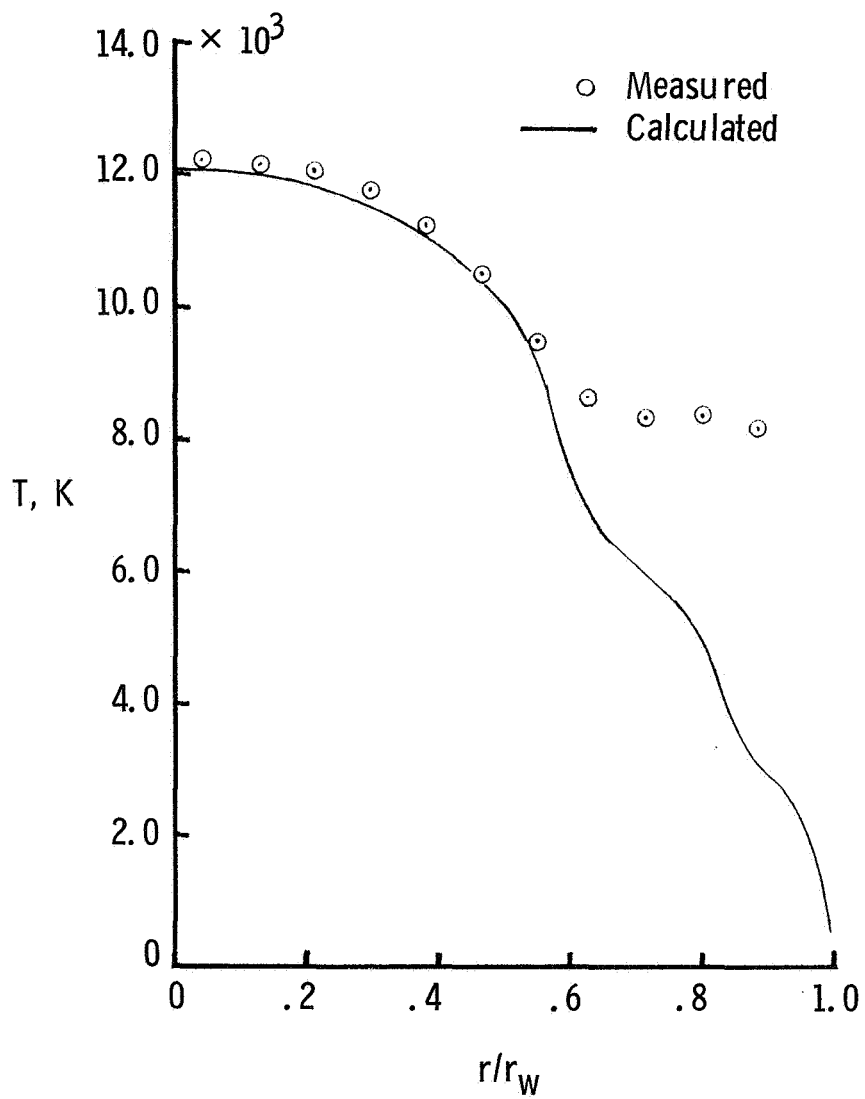


Figure 10.- Comparison of arc-heater temperature profile at  $z = 16$  cm.  
 $p_o = 0.40$  atm;  $I = 377$  amperes;  $\dot{m} = 4.8$  g/sec.



POSTMASTER: If Undeliverable (Section 158  
Postal Manual) Do Not Return

*"The aeronautical and space activities of the United States shall be conducted so as to contribute . . . to the expansion of human knowledge of phenomena in the atmosphere and space. The Administration shall provide for the widest practicable and appropriate dissemination of information concerning its activities and the results thereof."*

—NATIONAL AERONAUTICS AND SPACE ACT OF 1958

## NASA SCIENTIFIC AND TECHNICAL PUBLICATIONS

**TECHNICAL REPORTS:** Scientific and technical information considered important, complete, and a lasting contribution to existing knowledge.

**TECHNICAL NOTES:** Information less broad in scope but nevertheless of importance as a contribution to existing knowledge.

**TECHNICAL MEMORANDUMS:** Information receiving limited distribution because of preliminary data, security classification, or other reasons. Also includes conference proceedings with either limited or unlimited distribution.

**CONTRACTOR REPORTS:** Scientific and technical information generated under a NASA contract or grant and considered an important contribution to existing knowledge.

**TECHNICAL TRANSLATIONS:** Information published in a foreign language considered to merit NASA distribution in English.

**SPECIAL PUBLICATIONS:** Information derived from or of value to NASA activities. Publications include final reports of major projects, monographs, data compilations, handbooks, sourcebooks, and special bibliographies.

**TECHNOLOGY UTILIZATION PUBLICATIONS:** Information on technology used by NASA that may be of particular interest in commercial and other non-aerospace applications. Publications include Tech Briefs, Technology Utilization Reports and Technology Surveys.

Details on the availability of these publications may be obtained from:

SCIENTIFIC AND TECHNICAL INFORMATION OFFICE

NATIONAL AERONAUTICS AND SPACE ADMINISTRATION  
Washington, D.C. 20546